Real-Space Imaging of Triplon Excitations in Engineered Quantum Magnets

Robert Drost[1,*] Shawulienu Kezilebieke[2] Jose L. Lado[1] and Peter Liljeroth[1]

[1]*Aalto University, Department of Applied Physics, 00076 Aalto, Finland*
[2]*Department of Physics, Department of Chemistry and Nanoscience Center, University of Jyväskylä,
FI-40014 Jyväskylä, Finland*

Quantum magnets provide a powerful platform to explore complex quantum many-body phenomena. One example is triplon excitations, exotic many-body modes emerging from propagating singlet-triplet transitions. We engineer a minimal quantum magnet from organic molecules and demonstrate the emergence of dispersive triplon modes in one- and two-dimensional assemblies probed with scanning tunneling microscopy and spectroscopy. Our results provide the first demonstration of dispersive triplon excitations from a real-space measurement.

Quantum magnets provide a powerful platform to explore complex quantum many-body phenomena. In particular, many-body excitations in quantum magnets provide a playground to engineer emergent excitations only present in quantum materials [1–3]. Well-known examples are magnons [4] in ordered magnets and spinons [5,6] in quantum spin liquid systems. Both spinons and magnons emerge due to fluctuations of localized magnetic moments, and are associated with emergent quasiparticles with $S = 1/2$ or $S = 1$ appearing in the material. These two excitations have remained at the core of quantum magnetism, with a variety of methodologies and experimental techniques focused on distinguishing these modes in real experiments [7–10]. Quantum magnets can feature an additional more subtle type of excitation, emerging even when the individual building block of the quantum magnet is $S = 0$: The triplons.

Triplon excitations emerge from an internal excitation of each building block of the quantum magnet, going beyond the picture applicable to spinons and magnons [11–13]. When these internal singlet-triplet transitions in a quantum magnet become dispersive in the material, triplon modes emerge (see Fig. 1) [14–16]. Triplons are challenging to observe in conventional materials where either magnons or spinons are normally pursued. This stems from the fact that, for magnetic elements in bulk materials, the energy scales of singlet-triplet transitions is associated with Hund's energy, on the order of eV, and is dramatically larger than the typical bandwidth of spin fluctuations, on the order of meV [17]. Molecular systems [18], however, provide natural magnetic systems with competing ground states, including singlet-triplet transitions. This intrinsic competition, in stark contrast to bulk compounds, makes engineered molecular systems natural platforms to explore triplon excitations.

While triplon excitations have been studied in bulk compounds using, e.g., inelastic neutron scattering [19–23], they have not been experimentally observed on the atomic scale. Here, we show that triplon excitations can be produced in designer quantum systems and be probed in real-space using scanning tunneling microscopy (STM). We achieve this using metal phthalocyanine molecules, where the spin ground state can be tailored through the nature of the central metal atom and choice of substrate [24–28]. A recent study found cobalt phthalocyanine (CoPC) on
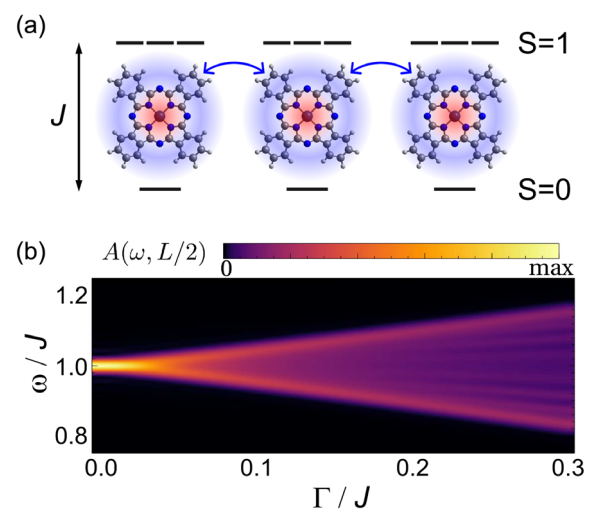

FIG. 1. Triplon excitations in a molecular spin chain. (a) CoPC on $NbSe_2$ hosts two unpaired electrons in different molecular orbital. The molecule has a singlet ground state, in which the electronic spins are antiparallel. Flipping one of the spins brings the molecule into the triplet state and creates a triplon. This fundamental excitation propagates through the chain through inter-molecular coupling. (b) Calculated triplon spectral function $A(\omega, L/2)$ for a molecular chain with $L = 20$ sites in the middle of the chain, as a function of the intermolecular coupling Γ.
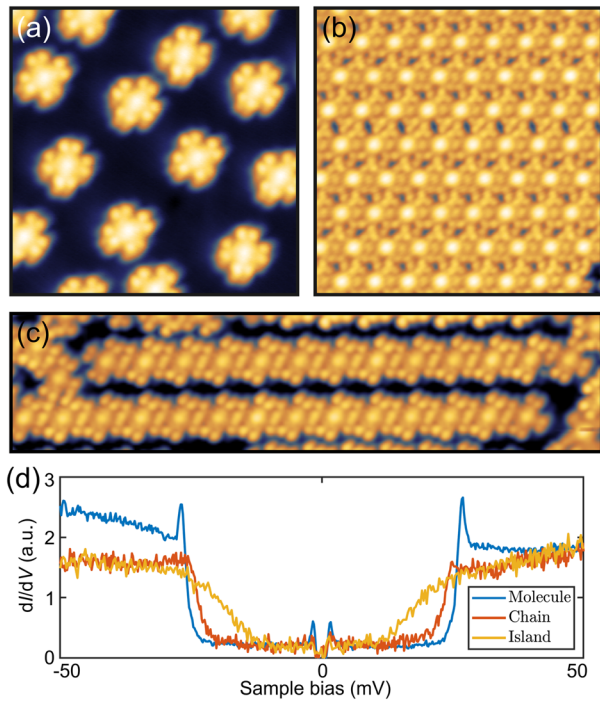
FIG. 2. CoPC molecules on $NbSe_2$. (a) CoPC adsorbs as individual molecules at low coverage. Image size 10×10 nm^2. Increasing the surface coverage yields molecular islands (b) and chains (c) self-assembly. Image sizes 12×12 nm^2 and 20×5 nm^2, respectively. (d) Conductance spectra acquired above the center atom of an individual CoPC (blue), a molecule in a chain (orange), and one in an island (yellow). The steplike features in the spectra correspond to spin excitations of the molecule by inelastic tunneling.

$NbSe_2$ to be in a singlet ground state, making it an ideal choice as a building block for structures with triplon excitations [28]. By designing both one-dimensional and two-dimensional molecular arrays, we demonstrate that dispersive triplons can be measured with inelastic spectroscopy. We further show that the dispersion bandwidth of triplons is strongly correlated with the dimensionality of the molecular assembly as expected from dispersive many-body modes. Our results provide a real-space demonstration of triplon modes in engineered molecular systems, suggesting this as a potential platform for realizing exotic many-body phenomena experimentally.

Figure 2 shows low-temperature STM images of CoPC molecules on the $NbSe_2$ substrate. The sample preparation is described in detail in the Supplemental Material [29]. Briefly, we sublime CoPc molecules onto a freshly cleaved $NbSe_2$ substrate under ultrahigh vacuum (UHV) conditions. Subsequently, the sample is inserted into a low-temperature STM operating at 4 K housed within the same UHV setup. All the dI/dV spectra shown here have been acquired with $NbSe_2$-coated superconducting tip [26]. CoPC on $NbSe_2$ self-assembles into various motifs depending on the surface coverage. Low coverage samples

yield individual molecules [Fig. 2(a)], while CoPC self-assembles into molecular chains (b) and islands (c) at higher coverage. As Wang and co-workers demonstrated recently [28], the molecule has two distinct adsorption sites on this surface. Depending on the alignment of the high-symmetry axes of molecule and substrate, it may display either Yu-Shiba-Rusinov states, or spin-flip excitations [26–28,37]. Here, we focus exclusively on the latter kind, as our aim is to engineer novel magnetic phases from an $S = 0$ ground state. The spin moments arise from two unpaired electrons occupying the molecular orbitals of CoPC. The two molecular orbitals, one located at the center of the molecule and another located in carbon atoms away from the center. Molecules in one- and two-dimensional (1D, 2D) assemblies exclusively display spin-flip excitations.

Figure 2(d) shows a representative conductance spectrum acquired above the metal center of an individual CoPC molecule in blue. Two features dominate the spectrum: The superconducting gap close to zero bias, and two sharp steps at higher energy. The superconducting gap arises from the $NbSe_2$ substrate and is not relevant for the spin-excitation features discussed here. The steps, placed symmetrically around the origin, are the characteristic signature of inelastic spin-flip excitations [28,38,39]. In this case, a tunneling electron with sufficient energy excites the spin system into the triplet state. The spectra have been acquired with a $NbSe_2$-coated superconducting tip [26] to enhance the energy resolution beyond the thermal limit [24,40]. This also results in a sharp peak at the edge of the spin-flip excitation steps arising from the superconducting density of states of the tip. Figure 2(d) also shows spectra acquired on molecules in chains or islands (shown in orange and yellow, respectively). These show a similar steplike feature, which is, however, shifted to significantly smaller energies while being considerably broader than on single molecules. The effect becomes more pronounced as we move from 1D assemblies to 2D islands.

The adsorption sites of CoPC are not commensurate with the $NbSe_2$ CDW reconstruction [41]. This creates locally different environments for each molecule, which has been previously shown to modulate the energies of YSR states of Fe atoms on $NbSe_2$ [42]. We observe that the location of the inelastic excitation steps varies by a few mV from one molecule to the next. These changes are likely due to adsorption-site driven changes to the molecular orbitals, affecting the exchange coupling inside each molecule depending on its surroundings [43,44]. This modulation in the step energy makes a quantitative analysis of the data on a molecule-by-molecule basis difficult. We therefore adopt a statistical approach and search for broader trends in a large dataset, which is summarized in Fig. 3. The data set consists of 713 conductance spectra of CoPC on $NbSe_2$, which we group into three categories depending on the adsorption geometry: Individual molecules [Fig. 3(a)], 1D chains [Fig. 3(b)], and 2D islands [Fig. 3(c)].
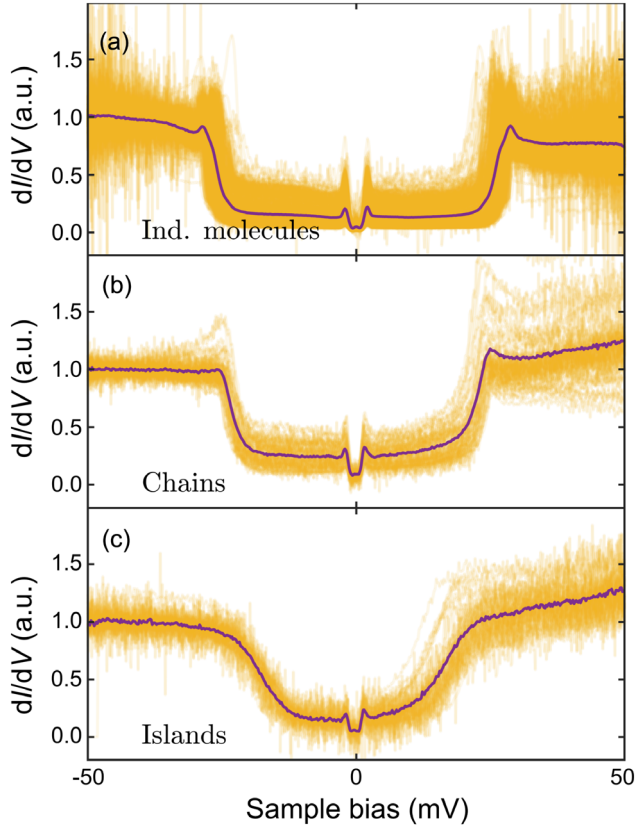
FIG. 3. Complete dataset used in our analysis. Conductance spectra acquired above (a) individual molecules, (b) molecules in chains, (c) molecules in islands, excluding edges. Purple lines are averages over all measurements in their respective class.
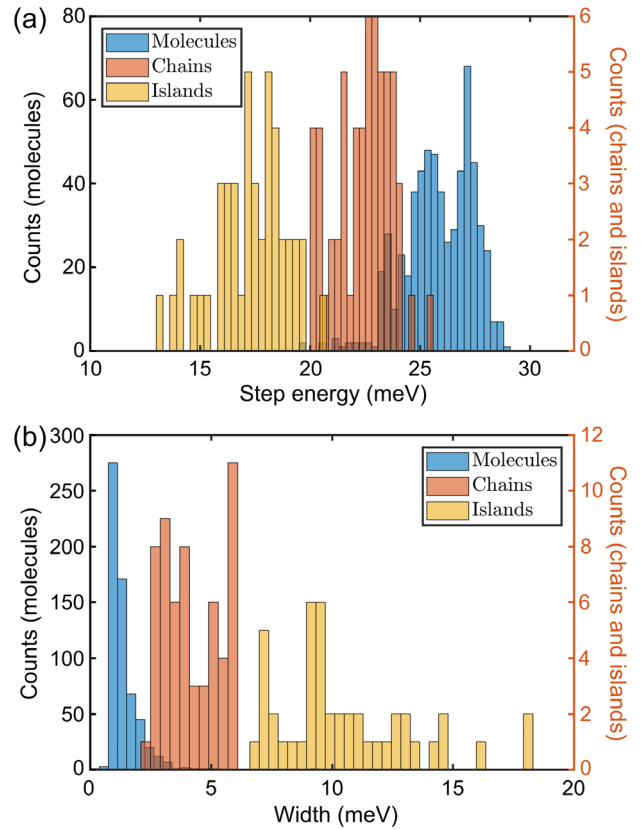

FIG. 4. Step energies and widths. Inelastic step energy (a) and width (b) extracted by our fitting procedure for individual molecules (blue), molecules in chains (orange), and islands (yellow). The spin excitation step moves to lower energy and broadens as the number of neighbor molecules increases.

We quantify the changes in the spectra by characterizing each spectrum by the location of the step and its width, by fitting them with a Fermi step function mirrored about the origin [29]. This method reliably extracts the center of the inelastic step, while the effective temperature of the fit function encodes all broadening mechanisms present in the experiment. The results of our analysis are summarized in Fig. 4. They quantify the trends already evident from the conductance spectra shown in Fig. 3. Individual molecules display by far the largest spin excitation gap of all molecular species. The multipeak distribution is likely due to interactions with the CDW. The excitation gap is significantly reduced for molecules in one- and two-dimensional assemblies [see Fig. 4(a)]. The more close neighbors surround a molecule, the lower the spin excitation energy becomes.

The position of the inelastic step may be influenced by a multitude of factors, and, in particular, solely by changes in the local environment [45–47]. A shift of the step energy is therefore not related with intermolecular spin-spin interactions. In addition to the step energy, the width of the inelastic step, shown in Fig. 4(b) increases when going from molecules to chains and islands. While individual molecules generally show values close to the expected thermal broadening at $T = 4.2$ K, data from one- and two-dimensional assemblies yields significantly larger values of the step width. The effect is more pronounced the more neighbors surround a given molecule.

Changes in the local adsorption geometry alone cannot explain this broadening of the inelastic step. Factors like anisotropy or other environmentally driven changes to the intramolecular exchange interaction do not affect the width of an excitation feature. The clear and consistent broadening of the inelastic step observed in our experiment is direct evidence of new intermolecular interactions and the formation of spin chains and lattices. The existence of these new couplings implies that excitations produced at any point in a structure can traverse it as triplons.

To support our findings, we build a model for spin chains mimicking the situation in our experiment. CoPC on NbSe$_2$ hosts two magnetic moments in different molecular orbitals [28]. One of those, labeled K, is located on the center ion, the second, labeled S, distributed over the outer ligands. Each site of our spin chain hence consists of a pair of spin operators K and S interacting through an intramolecular

exchange coupling J. The intermolecular exchange coupling Γ is driven by the spatial overlap of molecular orbitals at adjacent sites. The ligand orbitals will be the primary sources of intermolecular coupling [see sketch in Fig. 1(a)], leading to a Hamiltonian of the form

$$\mathcal{H} = \sum_i J_i \boldsymbol{S}_i \cdot \boldsymbol{K}_i + \Gamma \sum_{\langle i,j \rangle} \boldsymbol{S}_i \cdot \boldsymbol{S}_j. \qquad (1)$$

Here, $\boldsymbol{S}_i$ and $\boldsymbol{K}_i$ are spin-1/2 operators at lattice site i, J_i is the intramolecular exchange coupling at site i, Γ the intermolecular exchange coupling, and the sum $\langle i, j \rangle$ is taken over nearest neighbors. The spin-spectral function of the model $A(\omega, n) = \langle GS | K_n^z \delta(\omega - \mathcal{H} + E_{GS}) K_n^z | GS \rangle$ accounts for the singlet-triplet transition signaled by the inelastic step, and in particular is related with the differential conductance as $dI/dV(V, n) \sim \int_0^V A(V', n) dV'$. We solve the previous model using a tensor-network method and compute the spectral function with the kernel polynomial methodology [48–50]. Further details of the modeling are given in the Supplemental Material [29].

We simulate our experiment by computing the spin excitation spectrum at each lattice site and extracting the width of the resulting step. The distributions of step energies and widths is directly comparable to our experimental results, and we model the CDW-induced disorder by introducing random variations of the intramolecular coupling. In its simplest form, with $J_i = J$ and $\Gamma = 0$, the model produces a singlet-triplet excitation of energy J at each lattice site. This situation corresponds to an idealized scenario of individual molecules with no disorder. Keeping $\Gamma = 0$, but allowing for randomized variations of $J_i \in [J - \Delta_J/2, J + \Delta_J/2]$, produces shifts of the excitation energy between different sites as shown in Fig. 5(a). This stems from the fact that the singlet-triplet splitting is uniquely determined by the exchange Hund's coupling. This configuration [Fig. 5(a)] represents measurements on individual molecules in our experiment, where the width of the step remains unaffected by the variations of J_i. These results indeed reproduce with good accuracy the situation in our experiment: A broad distribution of excitation energies, but relatively uniform step widths [see Fig. 4(a)].

We now move on to the case with a finite coupling $\Gamma \neq 0$, considering first a pristine molecular chain with uniform Hund's coupling J [Fig. 5(b)]. In the bulk of the chain, as shown in Fig. 5(b), the broadening of the step converges to a fixed value dominated by the intermolecular coupling Γ. The coupling Γ acts as an effective broadening mechanism and increases the width of the step. This increased broadening accounts for the emergence of a triplon band [11]. The experimentally observed limit in the chains corresponds to a finite coupling Γ in the presence of small disorder in J, shown in Fig. 5(c). This limit is directly accounted for by taking $\langle J_i \rangle = J$ and $J_i \in [J - \Delta_J/2, J + \Delta_J/2]$. It is observed that
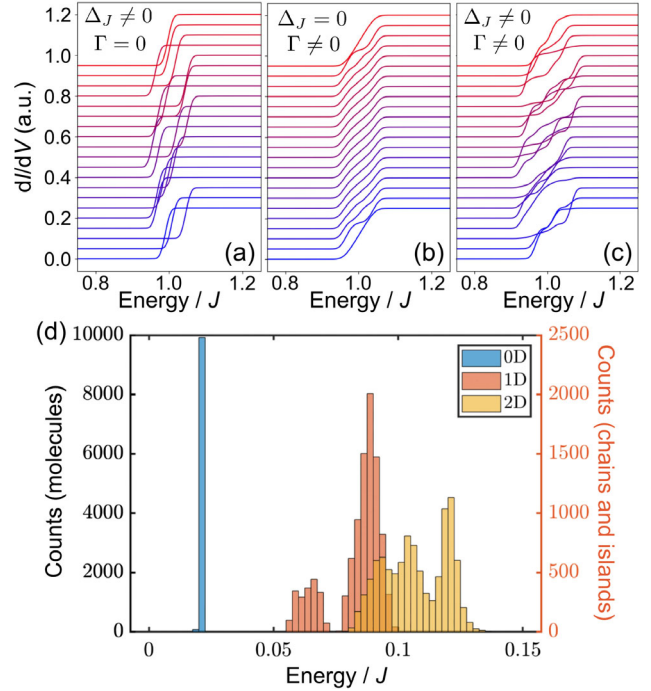

FIG. 5. Results from a spin model. (a)–(c) Simulated dI/dV curves in the absence of intermolecule coupling (a), and for coupled one-dimensional chain in the absence of disorder (b), and with disorder (c). (d) Distribution of the step widths obtained from our model, given in units of the exchange coupling J. The multimodal distributions in the 1D and 2D cases arise from the presence of edge and corner atoms. We took $\Gamma = 0.1J$ in (b),(c) [see Eq. (1)] and $\Delta_J = 0.1J$ in (a), (c).

the broadening of the steps remains, as in the pristine limit, but now with a slight shift of its onset driven by the different J_i.

We now evaluate our results using a statistical approach, considering both isolated molecules, chains and island as in the experiment. Figure 5(d) shows the step width obtained in our model in different lattice geometries. The simulated distributions are in good agreement with the experimental results: Starting from a narrow distribution for individual molecules, both the mean and the spread of values increase in the case of chains, and even further for islands. The simulations thus reproduce all essential aspects of our experiment. The increasing step width is directly related to a finite intermolecular spin-spin coupling with a typical value of $\Gamma \approx 8$ meV. The successive broadening of the inelastic feature we observe in tunneling spectroscopy is thus direct evidence of not only triplon formation, but also their propagation within molecular chains and islands. Arrays of CoPC on NbSe$_2$ thus form a minimal working example of a quantum magnet with a characteristic gapped spin excitation above the ground state. The model described by Eq. (1) is known to describe the effective spin dynamics of the Kondo insulators [51–53], tuning the intermolecular

interaction appropriately would enable the study of the quantum phase transition from the Kondo singlet to ordered antiferromagnetic phase in these systems.

The hunt for quantum magnets and exotic magnetic excitations has been mostly focused on magnetic insulators with complicated material chemistry and crystal structures. Our experiments show that arrays of metal-organic molecules are efficient platforms to simulate quantum magnets and study their excitations in a simplified setting. Magnetic molecules are adaptable model systems in which the magnetic interactions and ground state can be tuned through organic chemistry. Our Letter shows that they can form the building blocks of designer quantum magnets, offering a pathway to creating, exploring, and ultimately understanding magnetic excitations in quantum matter.

[*]Corresponding author.
robert.drost@aalto.fi

[1] S. Sachdev, Quantum magnetism and criticality, Nat. Phys. **4**, 173 (2008).

[2] A. Vasiliev, O. Volkova, E. Zvereva, and M. Markina, Milestones of low-D quantum magnetism, npj Quantum Mater. **3**, 18 (2018).

[3] M. Malki and G. S. Uhrig, Topological magnetic excitations, Europhys. Lett. **132**, 20003 (2020).

[4] A. V. Chumak, V. I. Vasyuchka, A. A. Serga, and B. Hillebrands, Magnon spintronics, Nat. Phys. **11**, 453 (2015).

[5] L. Faddeev and L. Takhtajan, What is the spin of a spin wave?, Phys. Lett. **85A**, 375 (1981).

[6] I. V. Kukushkin, J. H. Smet, V. W. Scarola, V. Umansky, and K. von Klitzing, Dispersion of the excitations of fractional quantum Hall states, Science **324**, 1044 (2009).

[7] Z. Hao and O. Tchernyshyov, Fermionic Spin Excitations in Two- and Three-Dimensional Antiferromagnets, Phys. Rev. Lett. **103**, 187203 (2009).

[8] T.-H. Han, J. S. Helton, S. Chu, D. G. Nocera, J. A. Rodriguez-Rivera, C. Broholm, and Y. S. Lee, Fractionalized excitations in the spin-liquid state of a kagome-lattice antiferromagnet, Nature (London) **492**, 406 (2012).

[9] M. Mourigal, M. Enderle, A. Klöpperpieper, J.-S. Caux, A. Stunault, and H. M. Rønnow, Fractional spinon excitations in the quantum Heisenberg antiferromagnetic chain, Nat. Phys. **9**, 435 (2013).

[10] B. D. Piazza, M. Mourigal, N. B. Christensen, G. J. Nilsen, P. Tregenna-Piggott, T. G. Perring, M. Enderle, D. F. McMorrow, D. A. Ivanov, and H. M. Rønnow, Fractional excitations in the square-lattice quantum antiferromagnet, Nat. Phys. **11**, 62 (2014).

[11] S. Sachdev and R. N. Bhatt, Bond-operator representation of quantum spins: Mean-field theory of frustrated quantum Heisenberg antiferromagnets, Phys. Rev. B **41**, 9323 (1990).

[12] N. Cavadini, G. Heigold, W. Henggeler, A. Furrer, H.-U. Güdel, K. Krämer, and H. Mutka, Magnetic excitations in the quantum spin system $TlCuCl_3$, Phys. Rev. B **63**, 172414 (2001).

[13] G. Xu, C. Broholm, Y.-A. Soh, G. Aeppli, J. F. DiTusa, Y. Chen, M. Kenzelmann, C. D. Frost, T. Ito, K. Oka, and H. Takagi, Mesoscopic phase coherence in a quantum spin fluid, Science **317**, 1049 (2007).

[14] P. A. McClarty, F. Krüger, T. Guidi, S. F. Parker, K. Refson, A. W. Parker, D. Prabhakaran, and R. Coldea, Topological triplon modes and bound states in a Shastry-Sutherland magnet, Nat. Phys. **13**, 736 (2017).

[15] S. Notbohm, P. Ribeiro, B. Lake, D. A. Tennant, K. P. Schmidt, G. S. Uhrig, C. Hess, R. Klingeler, G. Behr, B. Büchner, M. Reehuis, R. I. Bewley, C. D. Frost, P. Manuel, and R. S. Eccleston, One- and Two-Triplon Spectra of a Cuprate Ladder, Phys. Rev. Lett. **98**, 027403 (2007).

[16] K. Nawa, K. Tanaka, N. Kurita, T. J. Sato, H. Sugiyama, H. Uekusa, S. Ohira-Kawamura, K. Nakajima, and H. Tanaka, Triplon band splitting and topologically protected edge states in the dimerized antiferromagnet, Nat. Commun. **10**, 2096 (2019).

[17] J. M. Coey, *Magnetism and Magnetic Materials* (Cambridge University Press, Cambridge, England, 2010).

[18] E. Coronado, Molecular magnetism: From chemical design to spin control in molecules, materials and devices, Nat. Rev. Mater. **5**, 87 (2019).

[19] M. Kohno, O. A. Starykh, and L. Balents, Spinons and triplons in spatially anisotropic frustrated antiferromagnets, Nat. Phys. **3**, 790 (2007).

[20] C. Rüegg, B. Normand, M. Matsumoto, A. Furrer, D. F. McMorrow, K. W. Krämer, H. U. Güdel, S. N. Gvasaliya, H. Mutka, and M. Boehm, Quantum Magnets Under Pressure: Controlling Elementary Excitations in $TlCuCl_3$, Phys. Rev. Lett. **100**, 205701 (2008).

[21] J. Schlappa, T. Schmitt, F. Vernay, V. N. Strocov, V. Ilakovac, B. Thielemann, H. M. Rønnow, S. Vanishri, A. Piazzalunga, X. Wang, L. Braicovich, G. Ghiringhelli, C. Marin, J. Mesot, B. Delley, and L. Patthey, Collective Magnetic Excitations in the Spin Ladder $Sr_{14}Cu_{24}O_{41}$ Measured using High-Resolution Resonant Inelastic X-Ray Scattering, Phys. Rev. Lett. **103**, 047401 (2009).

[22] M. E. Zhitomirsky and A. L. Chernyshev, Colloquium: Spontaneous magnon decays, Rev. Mod. Phys. **85**, 219 (2013).

[23] M. E. Zayed, C. Rüegg, T. Strässle, U. Stuhr, B. Roessli, M. Ay, J. Mesot, P. Link, E. Pomjakushina, M. Stingaciu, K. Conder, and H. M. Rønnow, Correlated Decay of Triplet Excitations in the Shastry-Sutherland Compound $SrCu_2(BO_3)_2$, Phys. Rev. Lett. **113**, 067201 (2014).

[24] K. J. Franke, G. Schulze, and J. I. Pascual, Competition of superconducting phenomena and Kondo screening at the nanoscale, Science **332,** 940 (2011).

[25] L. Malavolti, M. Briganti, M. Hänze, G. Serrano, I. Cimatti, G. McMurtrie, E. Otero, P. Ohresser, F. Totti, M. Mannini, R. Sessoli, and S. Loth, Tunable spin–superconductor coupling of spin 1/2 vanadyl phthalocyanine molecules, Nano Lett. **18,** 7955 (2018).

[26] S. Kezilebieke, M. Dvorak, T. Ojanen, and P. Liljeroth, Coupled Yu-Shiba-Rusinov states in molecular dimers on NbSe$_2$, Nano Lett. **18,** 2311 (2018).

[27] S. Kezilebieke, R. Žitko, M. Dvorak, T. Ojanen, and P. Liljeroth, Observation of coexistence of Yu-Shiba-Rusinov states and spin-flip excitations, Nano Lett. **19,** 4614 (2019).

[28] Y. Wang, S. Arabi, K. Kern, and M. Ternes, Symmetry mediated tunable molecular magnetism on a 2D material, Commun. Phys. **4,** 103 (2021).

[29] See Supplemental Material at http://link.aps.org/supplemental/10.1103/PhysRevLett.131.086701, including Refs. [30–36], for further details.

[30] S. R. White, Density Matrix Formulation for Quantum Renormalization Groups, Phys. Rev. Lett. **69,** 2863 (1992).

[31] J. L. Lado and O. Zilberberg, Topological spin excitations in Harper-Heisenberg spin chains, Phys. Rev. Res. **1,** 033009 (2019).

[32] J. L. Lado and M. Sigrist, Solitonic in-gap modes in a superconductor-quantum antiferromagnet interface, Phys. Rev. Res. **2,** 023347 (2020).

[33] M. Ganahl, P. Thunström, F. Verstraete, K. Held, and H. G. Evertz, Chebyshev expansion for impurity models using matrix product states, Phys. Rev. B **90,** 045144 (2014).

[34] F. A. Wolf, I. P. McCulloch, O. Parcollet, and U. Schollwöck, Chebyshev matrix product state impurity solver for dynamical mean-field theory, Phys. Rev. B **90,** 115124 (2014).

[35] A. Weiße, G. Wellein, A. Alvermann, and H. Fehske, The kernel polynomial method, Rev. Mod. Phys. **78,** 275 (2006).

[36] N. Karjalainen, Z. Lippo, G. Chen, R. Koch, A. O. Fumega, and J. L. Lado, Hamiltonian inference from dynamical excitations in spin quantum dots, arXiv:2212.07893.

[37] M. Ternes, Spin excitations and correlations in scanning tunneling spectroscopy, New J. Phys. **17,** 063016 (2015).

[38] A. J. Heinrich, J. A. Gupta, C. P. Lutz, and D. M. Eigler, Single-atom spin-flip spectroscopy, Science **306,** 466 (2004).

[39] C. F. Hirjibehedin, C. P. Lutz, and A. J. Heinrich, Spin coupling in engineered atomic structures, Science **312,** 1021 (2006).

[40] S. H. Pan, E. W. Hudson, and J. C. Davis, Vacuum tunneling of superconducting quasiparticles from atomically sharp scanning tunneling microscope tips, Appl. Phys. Lett. **73,** 2992 (1998).

[41] M. M. Ugeda, A. J. Bradley, Y. Zhang, S. Onishi, Y. Chen, W. Ruan, C. Ojeda-Aristizabal, H. Ryu, M. T. Edmonds, H.-Z. Tsai, A. Riss, S.-K. Mo, D. Lee, A. Zettl, Z. Hussain, Z.-X. Shen, and M. F. Crommie, Characterization of collective ground states in single-layer NbSe$_2$, Nat. Phys. **12,** 92 (2015).

[42] E. Liebhaber, S. A. González, R. Baba, G. Reecht, B. W. Heinrich, S. Rohlf, K. Rossnagel, F. von Oppen, and K. J. Franke, Yu-Shiba-Rusinov states in the charge-density modulated superconductor NbSe$_2$, Nano Lett. **20,** 339 (2019).

[43] J. Bork, Y. hui Zhang, L. Diekhöner, L. Borda, P. Simon, J. Kroha, P. Wahl, and K. Kern, A tunable two-impurity Kondo system in an atomic point contact, Nat. Phys. **7,** 901 (2011).

[44] K. Yang, W. Paul, F. D. Natterer, J. L. Lado, Y. Bae, P. Willke, T. Choi, A. Ferrón, J. Fernández-Rossier, A. J. Heinrich, and C. P. Lutz, Tuning the Exchange Bias on a Single Atom from 1 mT to 10 T, Phys. Rev. Lett. **122,** 227203 (2019).

[45] D.-s. Wang, R. Wu, and A. J. Freeman, First-principles theory of surface magnetocrystalline anisotropy and the diatomic-pair model, Phys. Rev. B **47,** 14932 (1993).

[46] P. Gambardella, S. Stepanow, A. Dmitriev, J. Honolka, F. M. F. de Groot, M. Lingenfelder, S. S. Gupta, D. D. Sarma, P. Bencok, S. Stanescu, S. Clair, S. Pons, N. Lin, A. P. Seitsonen, H. Brune, J. V. Barth, and K. Kern, Supramolecular control of the magnetic anisotropy in two-dimensional high-spin Fe arrays at a metal interface, Nat. Mater. **8,** 189 (2009).

[47] B. W. Heinrich, L. Braun, J. I. Pascual, and K. J. Franke, Tuning the magnetic anisotropy of single molecules, Nano Lett. **15,** 4024 (2015).

[48] DMRGpy Library, https://github.com/joselado/dmrgpy.

[49] ITensor Library, http://itensor.org.

[50] M. Fishman, S. R. White, and E. M. Stoudenmire, The ITensor software library for tensor network calculations, SciPost Phys. Codebases 4 (2022), 10.21468/SciPostPhys-Codeb.4.

[51] P. Ram and B. Kumar, Theory of quantum oscillations of magnetization in Kondo insulators, Phys. Rev. B **96,** 075115 (2017).

[52] P. Ram and B. Kumar, Inversion and magnetic quantum oscillations in the symmetric periodic Anderson model, Phys. Rev. B **99,** 235130 (2019).

[53] J. Chen, E. M. Stoudenmire, Y. Komijani, and P. Coleman, Matrix product study of spin fractionalization in the 1D Kondo insulator, arXiv:2302.09701.